

Investigation of the Electron Transfer between Levodopa and Zinc Porphyrins at Bionic Interface

Yanru Fan¹, Bingxu Feng¹, Yu Huang^{1,*}, Xiaoquan Lu^{2,*}

¹ Key Laboratory of Hui Ethnic Medicine Modernization, Ministry of Education, Ningxia Engineering and Technology Research Center of Hui Medicine Modernization, College of Pharmacy, Ningxia Medical University, Yinchuan 750004, China

² Key Laboratory of Bioelectrochemistry & Environmental Analysis of Gansu Province, College of Chemistry & Chemical Engineering, Northwest Normal University, Lanzhou 730070, China

*E-mail: huangyunxmu@163.com, taaluxq@gmail.com

Received: 4 December 2017 / Accepted: 6 February 2018 / Published: 6 March 2018

In this paper, the interface between two immiscible electrolyte solutions (ITIES) is adopted as the bionic interface model to investigate the interfacial electron transfer (ET) process of levodopa by using thin-layer cyclic voltammetry. Three zinc porphyrins with a systematic variation in structure are used as the reactants in the organic phase for the supply of varied overall driving forces at the ITIES. The consecutive two-step ET reactions between levodopa and three zinc porphyrins with the corresponding ET rate constants are evaluated precisely. The relationship between the interfacial ET rate constants and the overall driving force are also studied. It is found that the ET kinetics of the bimolecular reactions at the ITIES obeys the Marcus theory in a wide potential region. The results of this work will assist in our understanding of the interfacial electron-transfer process of levodopa in vivo.

Keywords: levodopa; electron transfer; porphyrin; thin-layer cyclic voltammetry

1. INTRODUCTION

Levodopa (LD, 3,4-dihydroxy-l-phenylalanine or L-dopa) is one of the catecholamines and is a fascinating molecule that plays important roles in medicinal and biological chemistry, which is considered as the most effective treatment available for Parkinson's disease [1]. LD is the biological precursor of dopamine. LD can smoothly cross through the "blood brain barrier" as the molecular form due to its weaker alkalinity. Once it crosses, it is decarboxylated to dopamine (Fig. 1A) by the remaining dopamine terminals, and/or transformed by L-aromatic acid decarboxylase expressed by non-dopaminergic cells and terminals [2,3]. Hence, LD is directly involved in neurotransmission processes when using as a therapeutic drug.

According to the published reports [4-11], the redox or electron transfer (ET) process of LD has an effective role in the description of its properties. Electrochemical method is an effective method for the study of the redox and ET mechanisms of LD [12,13]. Brun and Rosset [14] reported the oxidation mechanism of LD in aqueous solution for the first time in 1974. They believed that the hydrolysis reaction in strong acidic pHs and intramolecular chemical reaction in neutral and basic pHs would occur after the oxidation of LD. Zare group [3] reported that the process of electrooxidation of LD in aqueous solution followed an $E_qC_iE_q$ mechanism. Rafiee et al. [15] studied the mechanism of LD reactions in the presence of nitrous acid/nitrite ion equilibria in mild acidic conditions by electrochemical methods. The results showed that the variation of reaction rates with pH was related to the variation of HNO_2 and NO_2^- percentage and protonation of the amine group of LD. They believed the predominance of intramolecular over intermolecular Michael addition. Afkhami et al. [16] reported the electrochemical oxidation processes of some catecholamines, including LD, in various pH values by using cyclic voltammetry. The observed homogeneous rate constants of cyclization reactions were also estimated. All above mentioned investigations referred to the redox or ET process of LD in homogeneous aqueous solution.

To the best of our knowledge, there is no study referring to the ET behavior of LD between two adjacent heterogeneous phases so far. One of the primary reasons lies in the difficulties in finding appropriate method to study the ET at the interface between two immiscible electrolyte solutions (ITIES). At present, three electrochemical methods have been used to investigate the ET at the ITIES, including four-electrode system [17], scanning electrochemical microscopy [18,19] and thin-layer cyclic voltammetry (TLCV) [20]. Wherein, TLCV became popular in the last decade for its simple operation and data analysis [21-23]. With the TLCV theory is further improved by our group [24,25], TLCV can be available to simultaneously evaluate the ET rate constants of multi-step ET reactions.

Because the ITIES is the simplest and most promising bionic interface model for the investigation of charge-transfer processes in biological systems, the ET behavior of LD at the ITIES is studied by using TLCV in this paper. Three zinc porphyrins with a systematic variation in structure are used as the reactants in the organic phase in order to supply the varied overall driving forces. The two-step ET reactions between LD and three zinc porphyrins with the corresponding ET rate constants are evaluated precisely. The relationship between the interfacial ET rate constants and the overall driving force are also discussed. The results of this work will assist in our understanding of the interfacial electron-transfer process of LD *in vivo*.

2. EXPERIMENTAL

2.1. Instrumentation

A CHI-900 electrochemical workstation (CH Instruments, Austin, TX) was employed for monitoring the consecutive ET at ITIES with a three-electrode cell that consisted of a pyrolytic graphite working electrode (EPG, area 0.3 cm^2), a saturated calomel reference electrode (SCE) and a platinum counter electrode. EPG was located in the organic thin layer while SCE and Pt electrode were

in the aqueous solution in the measurements. All the ET measurements were carried out at room temperature.

2.2. Chemicals

Levodopa was purchased from Aladdin Company without further purification. Sodium perchlorate (NaClO_4), sodium chloride (NaCl), nitrobenzene (NB) and tetrabutylammonium perchlorate (TBAClO_4) were used as received at AR or higher grade. The solutions were prepared with ultrapure water ($1.825 \times 10^7 \Omega \text{ cm}$) and were protected by nitrogen before use. Three zinc tetraarylporphyrins (ZnTArPs), including zinc-5,10,15,20-tetraphenylporphyrin (ZnTPP), zinc-5,10,15,20-tetranaphthalporphyrin (ZnTNP) and zinc-5,10,15,20-tetrapyrrenylporphyrin (ZnTPyP) were synthesized and characterized according to the reference [26].

2.3. Thin-layer cyclic voltammetry

The construction of NB/ H_2O interface was in accordance with references [29,31] except that the NB phase (2 μL) contained different zinc porphyrins. The concentration of ZnTArP was 1 mmol L^{-1} with TBAClO_4 (0.01 mol L^{-1}) as the supporting electrolyte in NB phase. LD was dissolved in aqueous solution using NaClO_4 (0.1 mol L^{-1}) and NaCl (0.1 mol L^{-1}) as supporting electrolyte. The quantitative theory of TLCV has been described in references [20,24,25] and the conclusive equation is shown as follows:

$$(i_{obs})^{-1} = d/(nFAc_{NB}^*D_{NB}) + (nFAc_{NB}^*)^{-1}(c_{H_2O}^*)^{-1}k_{et}^{-1} \quad (1)$$

$$c_{NB_n}^* = (i_{D_n}/i_{D_1}) \times c_{NB_1}^* \quad (n > 1) \quad (2)$$

$$0.5c_{NB_n}^* = (i_{D_n}/i_{D_1}) \times 0.6c_{NB_1}^* \quad (n > 1) \quad (3)$$

Wherein, i_{obs} is the observed plateau current, d is the thickness of the organic layer, n is the number of electron transferred, F stands for Faraday's constant, A is the geometrical area of working electrode, c_{NB}^* is the concentration of ZnTArP in the NB layer, D_{NB} stands for the diffusion coefficient of ZnTArP in NB, $c_{H_2O}^*$ is the reactant concentration in aqueous solution and k_{et} is the bimolecular reaction rate constant ($\text{cm s}^{-1} \text{ M}^{-1}$) between two reactants at the ITIES. $c_{NB_n}^*$ stands for the initial concentration of the reactant in NB for the n th ET. i_{D_n} is the steady-state diffusion limit current for the n th step ET. According to equation (1), the plot of $(i_{obs})^{-1}$ vs. $(c_{H_2O}^*)^{-1}$ should be a linear profile with the slope of $(nFAc_{NB}^*k_{et})^{-1}$ and intercept of $(i_D)^{-1}$, from which we can calculate k_{et} for each step ET.

2.4. Theoretical calculations

The molecular structure of LD is optimized by using density functional theory (DFT) at the B3LYP/6-31G(d) level. All calculations are performed with a Gaussian 09W software suite [27].

3. RESULTS AND DISCUSSION

3.1. Theoretical calculations

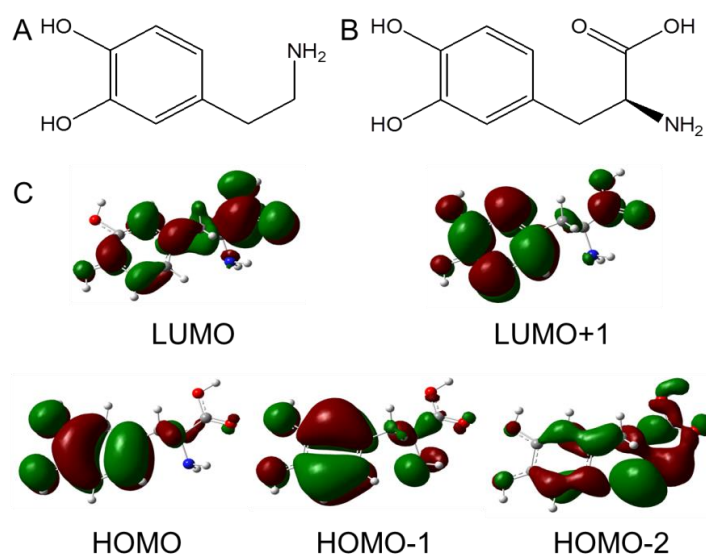


Figure 1. The structures of dopamine (A) and levodopa (B); The frontier molecular orbitals of levodopa (C). Calculated at the B3LYP/6-31G(d) level.

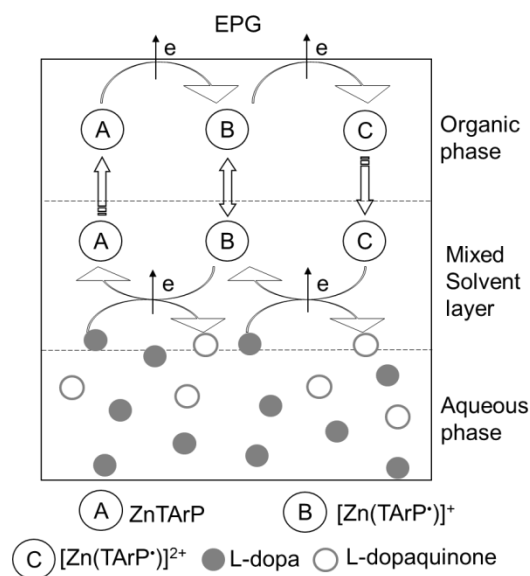
Table 1. The energy values of the molecular orbital of levodopa.

Molecular orbital	HOMO-2	HOMO-1	HOMO	LUMO	LUMO+1	LUMO+2	E_g^a
E/eV	-6.83	-6.27	-5.40	-0.05	0.34	0.64	5.35

a: $E_g = E_{LUMO} - E_{HOMO}$, Calculated at the DFT/ B3LYP/6-31G(d)level, Gaussian 09W software.

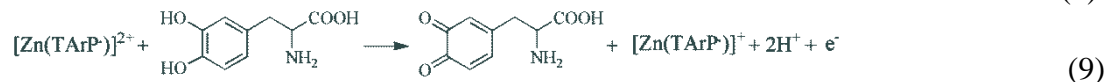
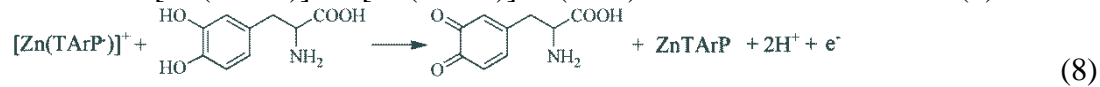
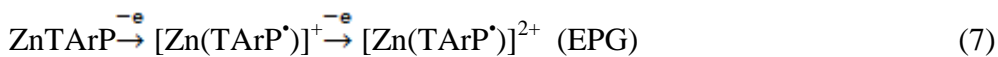
There is a catechol moiety carrying an alkyl sidechain with a carboxyl and an amine group on the sidechain in LD structure, as shown in Fig. 1B. Fig. 1C demonstrated the geometries and frontier orbitals of LD, which were calculated by DFT combined with Gaussian 09 software. The electron density at the highest occupied molecular orbital (HOMO) was mainly distributed over catechol moiety while the electron density at the lowest unoccupied molecular orbital (LUMO) was transferred from catechol moiety to alkyl sidechain. It could be concluded that the site of electron transfer was located in catechol moiety when HOMO was involved in chemical reactions. The data of molecular orbital energy and energy gap were listed in Table 1. The energy value increased from HOMO-2 to LUMO+2 and the energy gap was high up to 5.35 eV, suggesting that LD was easy to lose electrons and be oxidized.

3.3. Electron transfer of LD-ZnTArP reaction at the bionic interface



Scheme 1. Simplified consecutive electron transfer process between ZnTArP and levodopa at the NB/H₂O Interface.

The NB/H₂O interface was adopted as the bionic interface to investigate the interfacial electron transfer behavior of LD. Zinc porphyrins with a systematic structure variation were chosen as the reactants in organic layer in order to supply the varied overall driving forces. Scheme 1 showed the simplified consecutive electron transfer process between LD and ZnTArP at the NB/H₂O interface. ZnTArP was initially oxidized to [Zn(TArP•)]⁺ at suitable electrode potential. Then [Zn(TArP•)]⁺ diffused to the interface to accept the electrons from levodopa and ZnTArP was regenerated at the ITIES. Thus, the first ET step was completed between LD and [Zn(TArP•)]⁺ at the interface. Simultaneously, the remaining [Zn(TArP•)]⁺ was oxidized to [Zn(TArP•)]²⁺ at the EPG surface. [Zn(TArP•)]²⁺ was reduced by LD instantly when it diffused to the interface, which was the second ET step. The consecutive ET process might be described as following equations (7-9):



3.3.1. Investigation of the bimolecular ET reactions between LD and ZnTArPs by TLCV

The thin-layer protocol was employed to study two-step ET between ZnTArPs and LD at the ITIES. Fig. 3 showed the cyclic voltammograms of the electron transfer process between ZnTPP and LD. When the bare EPG was immersed into 1 mmol L⁻¹ LD solution involving 0.1 mol L⁻¹ NaCl and

0.1 mol L⁻¹ NaClO₄ as supporting electrolyte, a couple of reversible redox peaks of LD were observed with a formal potential at 419 mV, as shown in curve A.

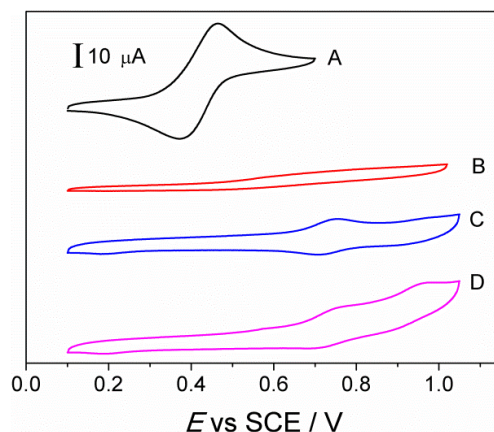


Figure 3. Thin layer cyclic voltammograms of electron transfer reaction between ZnTPP and levodopa at the NB/H₂O interface. A). Cyclic voltammogram of 1 mmol L⁻¹ levodopa at bare EPG. Supporting electrolyte: 0.1 mol L⁻¹ NaClO₄ + 0.1 mol L⁻¹ NaCl. B). The EPG surface was coated with 2 μL of NB. C). Cyclic voltammogram of a 2 μL NB solution containing 1 mmol L⁻¹ ZnTPP on the EPG surface. Supporting electrolyte: 0.01 mol L⁻¹ TBAClO₄. The aqueous solution only contained supporting electrolyte (0.1 mol L⁻¹ NaClO₄ + 0.1 mol L⁻¹ NaCl). D). Except for repeat of C, 1 mmol L⁻¹ levodopa was present in the aqueous phase. Scan rate was 5 mV s⁻¹.

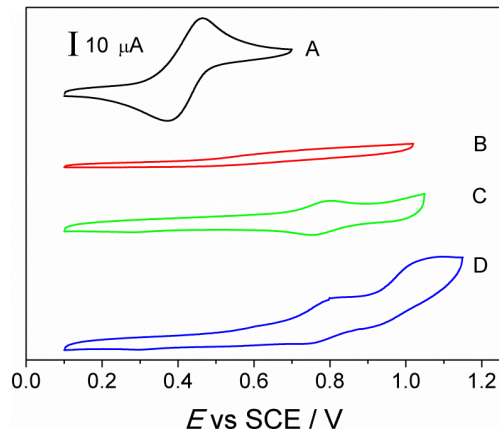


Figure 4. Thin layer cyclic voltammograms of electron transfer reaction between ZnTNP and Levodopa at the NB/H₂O interface. A). Cyclic voltammogram of 1 mmol L⁻¹ Levodopa at bare EPG. Supporting electrolyte: 0.1 mol L⁻¹ NaClO₄ + 0.1 mol L⁻¹ NaCl. B). The EPG surface was coated with 2 μL of NB. C). Cyclic voltammogram of a 2 μL NB solution containing 1 mmol L⁻¹ ZnTNP on the EPG surface. Supporting electrolyte: 0.01 mol L⁻¹ TBAClO₄. The aqueous solution only contained supporting electrolyte (0.1 mol L⁻¹ NaClO₄ + 0.1 mol L⁻¹ NaCl). D). Except for repeat of C, 1 mmol L⁻¹ Levodopa was present in the aqueous phase. Scan rate was 5 mV s⁻¹.

When the EPG was covered with NB (2 μL) solution to form a thin layer, the voltammetric response disappeared (Curve B, Fig. 3). It was because LD was separated from EPG surface by the

organic thin layer. When NB solution (2 μL) involving 1 mmol L^{-1} ZnTPP and 0.01 mol L^{-1} TBAClO₄ was injected onto the EPG surface without electroactive species in aqueous solution, curve C in Fig. 3 was gained. A pair of voltammetric waves at 733 mV corresponded to the apparent formal potential of the [Zn(TPP^{*})]⁺/Zn(TPP) couple. Based on above mentioned data, the difference between the formal potentials of LD and ZnTPP ($E_{\text{NB}}^f - E_{\text{H}_2\text{O}}^f = 314$ mV, shown in Table 2) was obtained, which was the overall driving force of the interfacial bimolecular reaction in this system [30]. When there was 1 mmol L^{-1} LD in the aqueous phase with 0.1 mol L^{-1} NaClO₄ and 0.1 mol L^{-1} NaCl as supporting electrolyte, an anodic current plateau (i_{obs}) was observed, as shown in curve D. The bimolecular redox reaction at the ITIES was at steady state.

Table 2. Two-step electron transfer rate constants of bimolecular reaction between levodopa and ZnTArP at the NB/H₂O Interface.

ET step	Bimolecular reaction system	$E_{\text{H}_2\text{O}}^f$ /mV ^a	E_{NB}^f /mV ^b	Driving force/ mV ^c	$k_{\text{et}}/\text{cm s}^{-1}\text{mol}^{-1}\text{L}$	$k_{\text{et}}^*/\text{cm s}^{-1}\text{mol}^{-1}\text{L}$
I	[Zn(TPP [*])] ⁺ - Levodopa	419	733	314	0.84	1.39
II	[Zn(TPP [*])] ²⁺ - Levodopa	419	923	504	4.72	9.43
I	[Zn(TNP [*])] ⁺ - Levodopa	419	776	357	1.10	1.83
II	[Zn(TNP [*])] ²⁺ - Levodopa	419	1002	583	3.59	7.18
I	[Zn(TPyP [*])] ⁺ - Levodopa	419	787	368	1.26	2.10
II	[Zn(TPyP [*])] ²⁺ - Levodopa	419	1029	610	2.76	5.52

a) The formal potential of levodopa in aqueous phase at the bare EPG. b) The formal potential of ZnTArP in organic phase. c) The driving force of the bimolecular reaction across the ITIES, ($E_{\text{NB}}^f - E_{\text{H}_2\text{O}}^f$). k_{et} is calculated from equation (1) and (2) while k_{et}^* is the corrected rate constant revised by equation (3). The values of k_{et}^* were reproducible within $\pm 10\%$ (n=3).

The consecutive ET between ZnTNP, ZnTPyP and LD were similar to that between ZnTPP and LD, as shown in Fig. 4 and Fig. 5.

According to equation (1), when c_{NB}^* is constant, $(i_{\text{obs}})^{-1}$ is linearly associated with $(c_{\text{H}_2\text{O}}^*)^{-1}$ and k_{et} can be obtained from the slope of $(nFAc_{\text{NB}}^*k_{\text{et}})^{-1}$. In the LD-ZnTPP ET system, the plots of i_{obs} vs. [LD] (A) and $(i_{\text{obs}})^{-1}$ vs. 1/[LD] (B) were presented in Fig. 6. With the increase of the concentration of LD in aqueous phase, the anodic plateau currents (i_{obs}) for two ET steps increased monotonically and i_{obs} would become concentration-independent because the current would be limited by diffusion of ZnTPP across the NB thin layer [31].

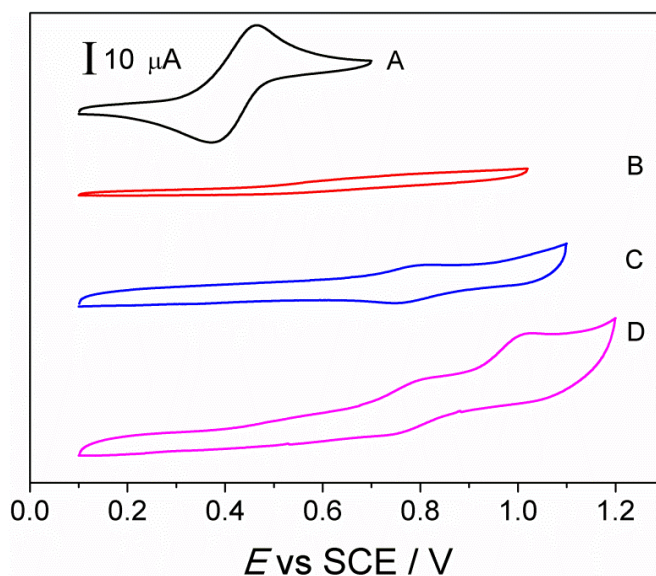


Figure 5. Thin layer cyclic voltammograms of electron transfer reaction between ZnTPyP and Levodopa at the NB/H₂O interface. A). Cyclic voltammogram of 1mmol L⁻¹ Levodopa at bare EPG. Supporting electrolyte: 0.1 mol L⁻¹ NaClO₄ + 0.1 mol L⁻¹ NaCl. B). The EPG surface was coated with 2μL of NB. C). Cyclic voltammogram of a 2μL NB solution containing 1 mmol L⁻¹ ZnTPyP on the EPG surface. Supporting electrolyte: 0.01 mol L⁻¹ TBAClO₄. The aqueous solution only contained supporting electrolyte (0.1 mol L⁻¹ NaClO₄ + 0.1 mol L⁻¹ NaCl). D). Except for repeat of C, 1mmol L⁻¹ Levodopa was present in the aqueous phase. Scan rate was 5 mV s⁻¹.

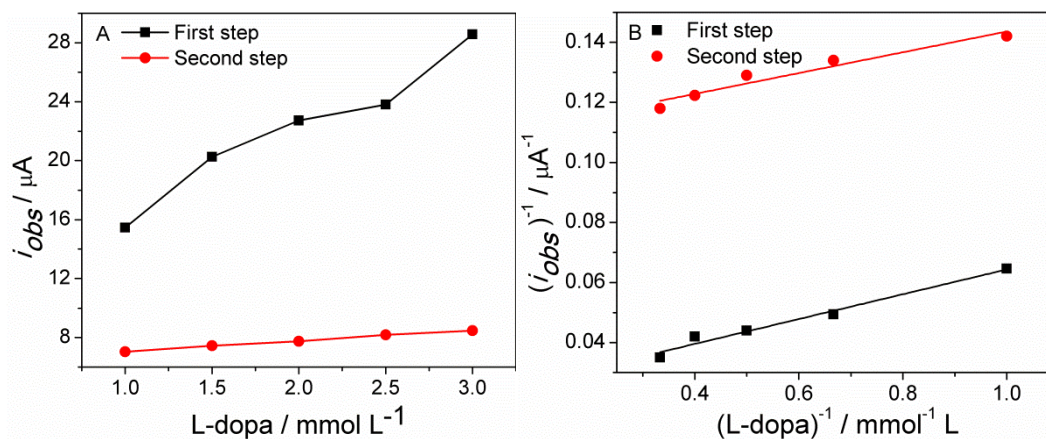


Figure 6. Variation of i_{obs} vs. the concentration of levodopa for ZnTPP-levodopa system (A). Variation of $(i_{obs})^{-1}$ vs. the reciprocal of the concentration of levodopa (B).

Fig. 6B showed well linear relationships of $(i_{obs})^{-1}$ vs. $[LD]^{-1}$, and k_{et} could be calculated by the slope of the linear equation, which were listed in Table 2. The graphs of i_{obs} vs. $[LD]$, and $(i_{obs})^{-1}$ vs. $[LD]^{-1}$ for ZnTNP-LD and ZnTPyP-LD systems were showed in Fig. 7 and Fig. 8, respectively.

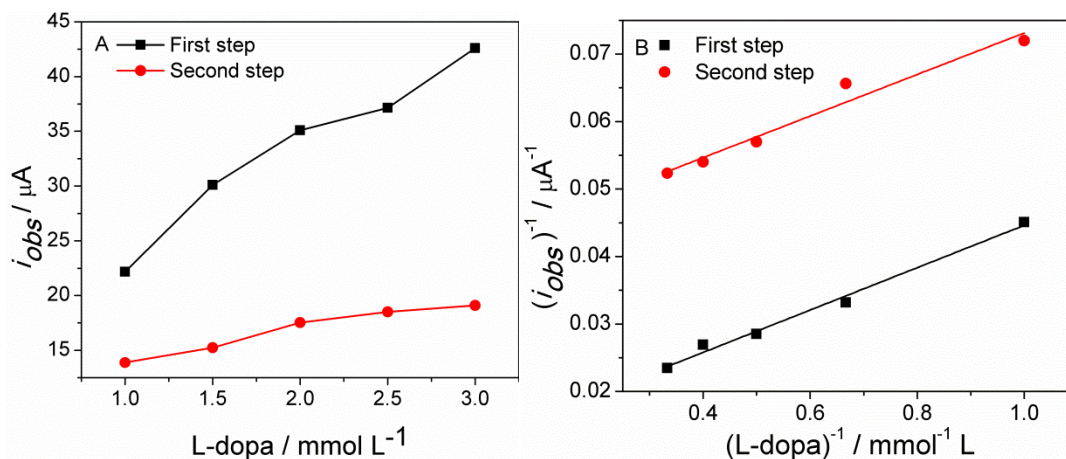


Figure 7. A) Variation of i_{obs} vs. the concentration of levodopa for ZnTNP-levodopa system. (B) Variation of $(i_{obs})^{-1}$ vs. the reciprocal of the concentration of levodopa.

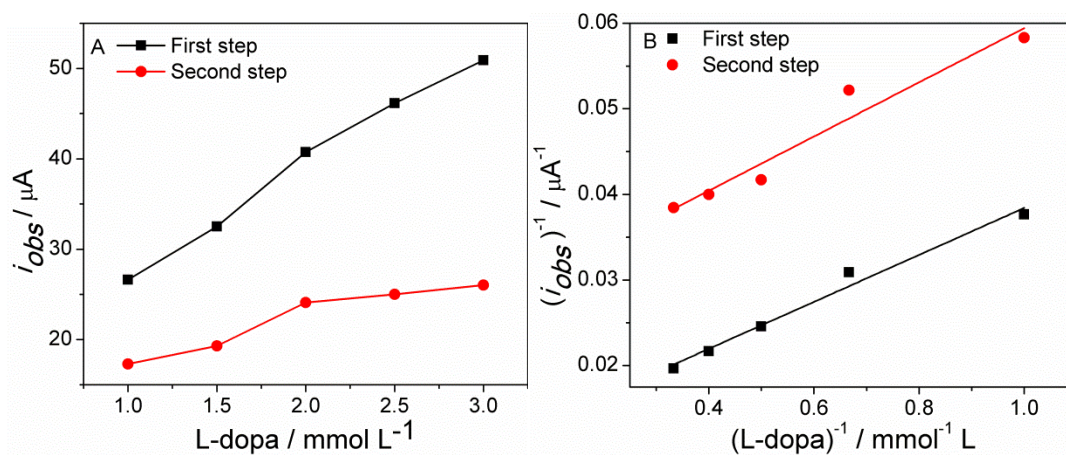


Figure 8. A) Variation of i_{obs} vs. the concentration of levodopa for ZnTPyP-levodopa system. (B) Variation of $(i_{obs})^{-1}$ vs. the reciprocal of the concentration of levodopa.

Shi and Anson [32] have demonstrated that the following two conditions must be met in order to obtain the reliable values for i_k and k_{et} : (i) i_{obs} must be significantly smaller than i_d , i.e. $i_{obs} \leq \sim 0.8i_d$ (otherwise, mass transport within the organic layer will dominate the obtained response), and (ii) the concentration of the reactant in the aqueous phase at the ITIES must not be significantly reduced from its value in the bulk of the solution by the cross-phase reaction (otherwise, mass-transport in the aqueous phase will affect the obtained response). Hence, the concentration of reactant in aqueous solution should meet the inequality (10), where t is the duration of plateau current flow:

$$\frac{4D_{NB}}{dk_{st}} \geq C_{H2O}^* \geq \frac{8 \times 10^3 c_{NB}^* D_{NB} t^{1/2}}{d(\pi D_{H2O})^{1/2}} \tag{10}$$

In the LD-ZnTNP ET system, the $i_{obs(I)}$ (15.5~28.6 μA) for the first step ET and the $i_{obs(II)}$ (7.0~8.5 μA) for the second step ET measured in Fig. 6 were below 34.7 μA ($0.8i_{d(I)}$) and 9.2 μA ($i_{d(II)}$) respectively, where i_d were calculated from equation (1-3). Similarly, the $i_{obs(I)}$ (22.2~42.6 μA) and the $i_{obs(II)}$ (13.9~19.1 μA) measured in Fig. 7 were below 60.5 μA ($0.8i_{d(I)}$) and 19.0 μA ($0.8i_{d(II)}$) respectively in the LD-ZnTNP ET system. The $i_{obs(I)}$ (26.6~50.9 μA) and the $i_{obs(II)}$ (17.3~26.0 μA)

measured in Fig. 8 were below $72.9 \mu\text{A}$ ($0.8i_{d(I)}$) and $28.8 \mu\text{A}$ ($0.8i_{d(II)}$) respectively in the LD-ZnTPyP ET system. In addition, the theoretical upper limit of $c_{\text{H}_2\text{O}}^*$ ([LD]) in the LD-ZnTPP ET system was calculated as 3.6 mmol L^{-1} from the inequality (10) using $D_{\text{ZnTPP}} = 8.5 \times 10^{-6} \text{ cm}^2 \text{ s}^{-1}$,²⁴ with $d = 6.7 \times 10^{-3} \text{ cm}$ (calculated for $2 \mu\text{L}$ of NB layered on the 0.3 cm^2 electrode) and $k_{\text{et}} \approx 1.4 \text{ cm s}^{-1} \text{ M}^{-1}$ (estimated as described in Table 2). The practical $c_{\text{H}_2\text{O}}^*$ ([LD]) in Fig. 6 ranged from 1.0 to 3.0 mmol L^{-1} , which was in well accordance with the constraint inequality (10). The suitable experiment conditions guaranteed the reliability of the obtained k_{et} data.

3.3.2. The relationship between driving force and ET rate constant at the ITIES

The relationship between interfacial ET rate constant (k_{et}) and overall driving force is one of the key problems during the interfacial ET process. The overall driving force is composed of the difference between the formal potentials of the redox couples in adjacent two phases (ΔE^0) and the Galvani potential difference ($\Delta_w^0 \phi$), as shown in equation (11) [30,33]:

$$\Delta E_{1/2} = \Delta E^0 + \Delta_w^0 \phi \quad (11)$$

The correlation between the ET rate constant (k_{et}) of a second-order ET and the activation energy (ΔG^\ddagger) can be written as equation (12) [30,34]:

$$k_{\text{et}} = \text{const exp}(-\Delta G^\ddagger / RT) \quad (12)$$

For a lower overpotential, a Butler-Volmer model approximation can be employed as follows [35]:

$$\Delta G^\ddagger = -\alpha F(\Delta E^0 + \Delta \phi) \quad (13)$$

where α is the transfer coefficient and F is the Faraday constant. According to the Marcus theory, the activation energy for an ET reaction can be described in equation (14) when the overpotential is high:

$$\Delta G^\ddagger = (\lambda/4)(1 + \Delta G^0/\lambda)^2 \quad (14)$$

where λ is the reorganization energy, and ΔG^0 is obtained by

$$\Delta G^0 = -F(\Delta E^0 + \Delta \phi) \quad (15)$$

In this work, $\Delta_w^0 \phi$ was kept constant by using a certain concentration of potential-determining ion ($[\text{ClO}_4^-]$) while ΔE^0 was adjusted by varying redox couple in the organic phase. Hence, ΔE^0 was the dominating factor which influenced the overall driving force.

Fig. 9 showed the dependence of $\log k_{\text{et}}^*$ on the driving force ($\Delta E_{1/2}$) among three bimolecular reaction systems. At lower driving force ($\Delta E_{1/2} < 368 \text{ mV}$), the values of $\log k_{\text{et}}^*$ for the first step ET gradually increased with the increase of the driving force. In contrast, the values of $\log k_{\text{et}}^*$ for the second step ET decreased when the driving force exceeded 583 mV . These behaviors can only be explained by the Marcus theory. Marcus theory predicts that the rate constant of an ET reaction increases when the driving force is low and decreases when the driving force is high [36,37]. Bard group [30,38] and Shao et al. [35] have verified the existence of a Marcus inverted region for an ET reaction at an ITIES by scanning electrochemical microscopy. Girault et al. [39] have observed the Marcus inverted region for a photoinduced ET at a polarized ITIES. Our group [40] investigated the ET reaction between iron porphyrins with varied substitutes and benzoquinone at an ITIES by

scanning electrochemical microscopy, in which the Marcus inverted region was also observed. It should be noted that the relationship between driving force and ET rate constant for LD-ZnTArP reactions in this work was completely different from that for ZnTArP- $\text{Fe}(\text{CN})_6^{4-}$ reactions in our previous work [41], though the identical zinc porphyrins were used in the organic phase in two works. In our previous work, the classic redox couple ($\text{Fe}(\text{CN})_6^{3-}$ - $\text{Fe}(\text{CN})_6^{4-}$) was chosen in aqueous phase to investigate the effect of the systematic structure variation of zinc porphyrins on their interfacial ET kinetics and the redox behaviors. It was found that the two-step ET rate was insensitive to the change of the driving force in a wide potential region for ZnTArP- $\text{Fe}(\text{CN})_6^{4-}$ reaction systems. It could be concluded that the ET kinetics of a bimolecular reaction at the ITIES was crucially affected by the reactant species in two adjacent phases by comparison of the two works.

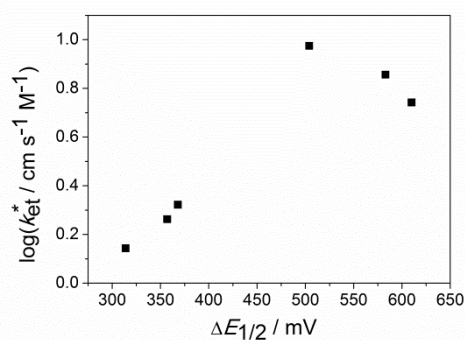


Figure 9. The dependence of $\log k_{\text{et}}^*$ on the driving force among three ZnTArP-levodopa systems.

4. CONCLUSION

The NB/ H_2O interface is used as the bionic interface for investigation of the interfacial ET behavior of levodopa in this work. The bimolecular reactions between levodopa and three zinc porphyrins are evaluated by using TLCV. The two-step ET rate constants are also calculated precisely. The correlation between the two-step ET rate constants and the overall driving force are discussed in detail. The results show that the values of $\log k_{\text{et}}^*$ for the first step ET gradually increase while that of the second step ET decrease in a wide potential range, where the Marcus inverted region is observed. The results of this work could make contributions for our understanding of the electron-transfer process of levodopa across the biomembrane in vivo.

ACKNOWLEDGMENTS

This work was supported by the Natural Science Foundation of China (Grant Nos. 21327005, 21575115, 21362026), Ningxia Youth Science and Technology Talent Supporting Engineering, Ningxia Medical University Special Talent Startup Project (XT2016004). The authors thank Dr. Xiaojie Jin, Prof. Xiaojun Yao (Lanzhou University) for their help in theoretical calculations.

References

1. M. Jaber, and J. F. Lambert, *J. Phys. Chem. Lett.*, 1 (2010) 85.

2. S. Shahrokhian, and E. Asadian, *J. Electroanal. Chem.*, 636 (2009) 40.
3. M. Eslami, M. Namazian, and H. R. Zare, *Electrochim. Acta*, 88 (2013) 543.
4. D. Dimić, D. Milenković, J. Dimitrić Marković, and Z. Marković, *Phys. Chem. Chem. Phys.*, 19 (2017) 12970.
5. M. Mazloun-Ardakani, E. Amin-sadrabadi, A. Khoshroo, and M. Salavati-Niasari, *J. Inorg. Organomet. Polym. Mater.*, 25 (2015) 1576.
6. M. Mazloun-Ardakani, A. Khoshroo, and L. Hosseinzadeh, *Sens. Actuators, B*, 204 (2014) 282.
7. Y. Shoja, A. A. Rafati, and J. Ghodsi, *Mater. Sci. Eng., C*, 58 (2016) 835.
8. K. Jodko-Piorecka, and G. Litwinienko, *Free Radical Biol. Med.*, 83 (2015) 1.
9. M. Mazloun-Ardakani, M. Yavari, M. A. Sheikh-Mohseni, and B. F. Mirjalili, *Catal. Sci. Technol.*, 3 (2013) 2634.
10. K. Reddaiah, T. M. Reddy, and P. Raghu, *J. Electroanal. Chem.*, 682 (2012) 164.
11. N. F. Atta, S. M. Ali, E. H. El-Ads, and A. Galal, *J. Electrochem. Soc.*, 160 (2013) G3144.
12. V. K. Gupta, R. Jain, K. Radhapyari, N. Jadon, and S. Agarwal, *Anal. Biochem.*, 408 (2011) 179.
13. X. K. Xu, Z. H. Zhu, N. Liu, Y. F. Li, X. Li, L. Liu, M. Lin, and J. G. Wang, *J. Electrochem. Soc.*, 163 (2016) H757.
14. A. Brun, and R. Rosset, *J. Electroanal. Chem.*, 49 (1974) 287.
15. M. Rafiee, and L. Khalafi, *Electrochim. Acta*, 55 (2010) 1809.
16. A. Afkhami, D. Nematollahi, L. Khalafi, and M. Rafiee. *Int. J. Chem. Kinet.*, 37 (2005) 17.
17. Z. Samec, V. Marecek, and J. Weber, *J. Electroanal. Chem.*, 96 (1978) 245.
18. T. Solomont, and A. J. Bard, *J. Phys. Chem.*, 99 (1995) 17487.
19. C. Wei, A. J. Bard, and M. V. Mirkin, *J. Phys. Chem.*, 99 (1995) 16033.
20. C. Shi, and F. C. Anson, *Anal. Chem.*, 70 (1998) 3114.
21. J. Xu, A. Frcic, J. A. C. Clyburne, R. A. Gossage, and H. Z. Yu, *J. Phys. Chem. B*, 108 (2004) 5742.
22. R. Wang, T. Okajima, F. Kitamura, N. Matsumoto, T. Thiemann, S. Mataka, and T. Ohsaka, *J. Phys. Chem. B*, 107 (2003) 9452.
23. Y. C. Li, E. M. W. Tsang, A. Y. C. Chan, and H. Z. Yu, *Electrochem. Commun.*, 8 (2006) 951.
24. X. Q. Lu, P. Sun, D. N. Yao, B. W. Wu, Z. H. Xue, X. B. Zhou, R. P. Sun, L. Li, and X. H. Liu, *Anal. Chem.*, 82 (2010) 8598.
25. X. Q. Lu, Y. Li, P. Sun, B. W. Wu, Z. H. Xue, X. H. Liu, and X. B. Zhou, *J. Phys. Chem. C*, 116 (2012) 16660.
26. Y. R. Fan, Y. Huang, Y. Jiang, X. M. Ning, X. M. Wang, D. L. Shan, and X. Q. Lu, *J. Colloid Interface Sci.*, 462 (2016) 100.
27. M. J. Frisch, G. W. Trucks, H. B. Schlegel, G. E. Scuseria, M. A. Robb, J. R. Cheeseman, G. Scalmani, V. Barone, B. Mennucci, G. A. Petersson, H. Nakatsuji, M. Caricato, X. Li, H. P. Hratchian, A. F. Izmaylov, J. Bloino, G. Zheng, J. L. Sonnenberg, M. Hada, M. Ehara, K. Toyota, R. Fukuda, J. Hasegawa, M. Ishida, T. Nakajima, Y. Honda, O. Kitao, H. Nakai, T. Vreven, J. A. Montgomery Jr., J. E. Peralta, F. Ogliaro, M. Bearpark, J. J. Heyd, E. Brothers, K. N. Kudin, V. N. Staroverov, R. Kobayashi, J. Normand, K. Raghavachari, A. Rendell, J. C. Burant, S. S. Iyengar, J. Tomasi, M. Cossi, N. Rega, J. M. Millam, M. Klene, J. E. Knox, J. B. Cross, V. Bakken, C. Adamo, J. Jaramillo, R. Gomperts, R. E. Stratmann, O. Yazyev, A. J. Austin, R. Cammi, C. Pomelli, J. W. Ochterski, R. L. Martin, K. Morokuma, V. G. Zakrzewski, G. A. Voth, P. Salvador, J. J. Dannenberg, S. Dapprich, A. D. Daniels, O. Farkas, J. B. Foresman, J. V. Ortiz, J. Cioslowski, and D. J. Fox, Gaussian 09, Revision A.01, Gaussian, Inc., Wallingford CT, 2009.
28. M. Arvand, and N. Ghodsi, *J. Solid State Electrochem.*, 17 (2013) 775.
29. S. Shahrokhian, and E. Asadian, *J. Electroanal. Chem.*, 636 (2009) 40.
30. M. Tsionsky, A. J. Bard, and M. V. Mirkin, *J. Am. Chem. Soc.*, 119 (1997) 10785.

31. C. Shi, and F. C. Anson, *J. Phys. Chem. B*, 102 (1998) 9850.
32. C. Shi, and F. C. Anson, *J. Phys. Chem. B*, 105 (2001) 1047.
33. J. R. Miller, L. T. Calcaterra, and G. L. Closs, *J. Am. Chem. Soc.*, 106 (1984) 3047.
34. Z. Ding, B. M. Quinn, and A. J. Bard, *J. Phys. Chem. B*, 105 (2001) 6367.
35. P. Sun, F. Li, Y. Chen, M. Q. Zhang, Z. Q. Zhang, Z. Gao, and Y. H. Shao, *J. Am. Chem. Soc.*, 125 (2003) 9600.
36. R. A. Marcus, *J. Phys. Chem.*, 94 (1990) 4152.
37. R. A. Marcus, *J. Phys. Chem.*, 95 (1991) 2010.
38. Y. Zu, F. Fan, and A. J. Bard, *J. Phys. Chem. B*, 103 (1999) 6272.
39. N. Eugster, D. J. Fermin, and H. H. Girault, *J. Phys. Chem B*, 106 (2002) 3428.
40. X. Q. Lu, W. T. Gu, R. P. Sun, and X. H. Liu, *Electroanalysis*, 24 (2012) 2341.
41. Y. R. Fan, Y. Huang, S. X. Wang, Y. Jiang, D. L. Shan, and X. Q. Lu, *Electrochim. Acta*, 190 (2016) 419.

© 2018 The Authors. Published by ESG (www.electrochemsci.org). This article is an open access article distributed under the terms and conditions of the Creative Commons Attribution license (<http://creativecommons.org/licenses/by/4.0/>).